



HAL
open science

Integrated process for the removal of indoor VOCs from food industry manufacturing Elimination of Butane-2,3-dione and Heptan-2-one by cold plasma-photocatalysis combination

W. Abou Saoud, A.A. Assadi, A. Kane, A.-V. Jung, Pierre Le Cann, A. Gerard, F. Bazantay, A. Bouzaza, D. Wolbert

► To cite this version:

W. Abou Saoud, A.A. Assadi, A. Kane, A.-V. Jung, Pierre Le Cann, et al.. Integrated process for the removal of indoor VOCs from food industry manufacturing Elimination of Butane-2,3-dione and Heptan-2-one by cold plasma-photocatalysis combination. *Journal of Photochemistry and Photobiology A: Chemistry*, 2020, 386, pp.112071. 10.1016/j.jphotochem.2019.112071 . hal-02309962

HAL Id: hal-02309962

<https://univ-rennes.hal.science/hal-02309962>

Submitted on 27 May 2020

HAL is a multi-disciplinary open access archive for the deposit and dissemination of scientific research documents, whether they are published or not. The documents may come from teaching and research institutions in France or abroad, or from public or private research centers.

L'archive ouverte pluridisciplinaire **HAL**, est destinée au dépôt et à la diffusion de documents scientifiques de niveau recherche, publiés ou non, émanant des établissements d'enseignement et de recherche français ou étrangers, des laboratoires publics ou privés.

**Integrated process for the removal of indoor VOCs from food
industry manufacturing: elimination of Butane-2,3-dione and
Heptan-2-one by cold plasma-photocatalysis combination**

Wala Abou Saoud¹, Aymen Amine Assadi^{1*}, Abdoulaye Kane², Aude-Valerie Jung²,
Le Cann Pierre³, Anne Gerard³, Frederic Bazantay⁴, Abdelkrim Bouzaza¹, Dominique
Wolbert¹

¹Laboratoire Sciences Chimiques de Rennes - équipe Chimie et Ingénierie des Procédés, UMR 6226
CNRS, ENSCR-11, allée de Beaulieu, CS 508307-35708 Rennes, France.

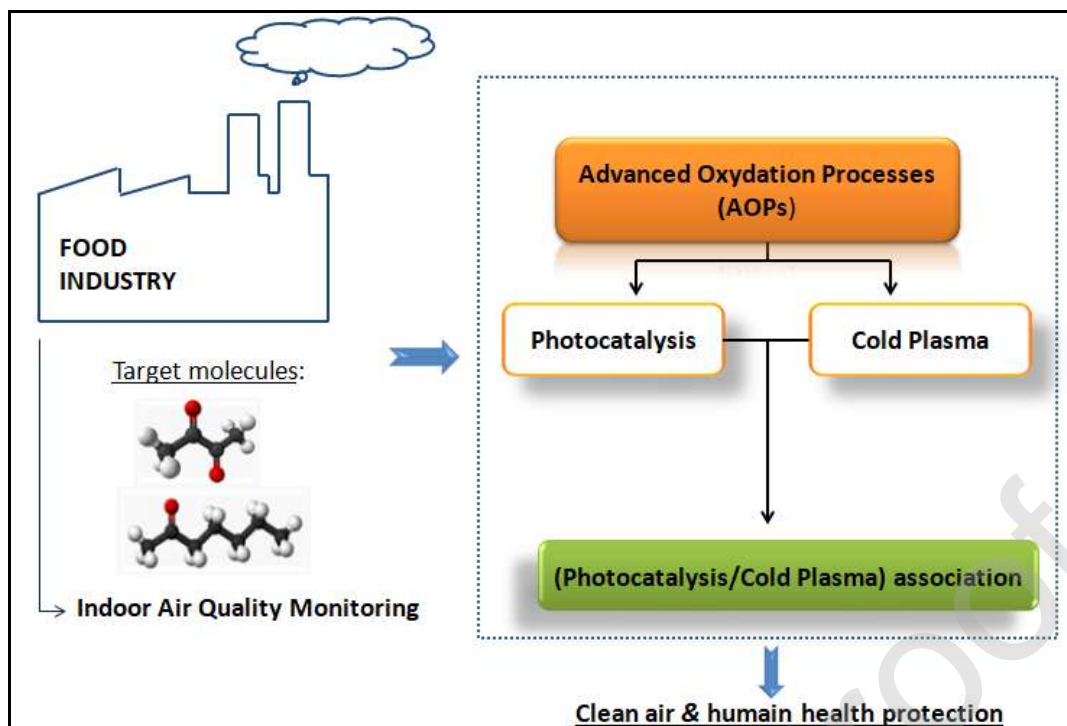
²UniLaSalle-Ecole des Métiers de l'Environnement (UniLaSalle-EME), Campus de Ker Lann, avenue
Robert Schuman Bruz, France.

³Univ Rennes, Inserm, EHESP, Irset (Institut de recherche en santé, environnement et travail)-
UMR_S 1085, F-35000 Rennes, France.

⁴Pôle Cristal, 49 Avenue René Cassin, 22100 Dinan.

* Corresponding authors. E-mails: aymen.assadi@ensc-rennes.fr (A. Assadi); Tel.: +33 2 23 23 81 52.

Graphical abstract



Highlights

- Plasma catalysis association for indoor air treatment has been investigated.
- Synergetic effect between plasma and catalysis has been confirmed
- Good performance on combination of photocatalysis to plasma technologies.
- Mineralization and oxidize by-products of a binary mixture were monitored.

Abstract

Coupling Non-thermal plasma (dielectric barrier discharge) with photocatalysis (TiO_2 - /UV) can be a promising technique to improve indoor air quality. In this study, Butane-2,3-dione and Heptan-2-one, usually found in food industry, were used as target compounds. Firstly, each pollutant was studied alone by photocatalytic treatment under experimental parameter effects like gases flow rate, VOCs inlet concentration, and humidity levels. Otherwise, in order to understand pollutants

reaction mechanisms, a complex composition mixture was then studied and discussed. Experiments with dry and wet air showed good Heptan-2-one removal but negatively affected Butane-2,3-dione elimination rate. The Butane-2,3-dione/Heptan-2-one oxidation study was carried out by cold plasma-photocatalysis combination in the same pilot reactor. Excellent treatment yields were observed in terms of pollutant removal efficiency, mineralization and Ozone decomposition. Additionally, intermediate by-product exhausts from three technologies e.g. TiO₂/UV-light system, DBD-plasma and their combination are identified.

Keywords: indoor air of food industry, Butane-2,3-dione/Heptan-2-one mixture, (photocatalysis-DBD plasma) association, synergetic effect.

1. Introduction

Volatile Organic Compounds (VOCs) e.g. ketones, aldehydes and BTEX (Benzene, Toluene, Ethylbenzene and Xylenes), are one of the most significant groups of indoor air pollutants [1,2]. Some odorous compounds such as Butane-2,3-dione and Heptan-2-one, emitted during food processing and preparation can be responsible for olfactory pollution [3], and are hazardous to health which can present a damage for overall human exposure to polluted environments. Therefore, removing/destroying VOCs emitted from dietary sectors is a major issue. Promising technologies, namely Advanced Oxidation Processes (AOPs), more efficient to treat organic compounds resistant to conventional processes, are under development and can provide interesting solutions in air control. AOPs such as photocatalysis [4,5], cold plasma [2,6-8] and catalytic ozonation [9,10], based on ozone and/or free reactive species (atomic oxygen, peroxide ions and hydroxyl radicals), appear as innovative

technologies to overcome limitations encountered by traditional processes. However, each method used alone can present some limitations: (i) accumulation of residues on the catalyst surface leads to a gradual decrease in photocatalytic activity, which regularly requires a regeneration step [11-13] and (ii) a low CO₂ selectivity was observed via plasma treatment and also (iii) undesirable by-product formation (carbon monoxide CO and ozone O₃) [14,15], each of them constitutes significant limitations which limit single mode usage. Therefore, it is better to associate photocatalysis and plasma together to ensure (i) high treatment efficiency and (ii) overcome existing disadvantages [16-22]. In this context, several studies have focused on the oxidation of VOCs via photocatalysis-plasma technologies and reported that an enhancement of more than 10% was observed on removal efficiency of malodorous pollutant exhaust from animal quartering centers like ammonia (NH₃), dimethyl disulfide (CH₃SSCH₃) and butyraldehyde (C₄H₈O) [12,18]. In this work, a commercial Glass Fiber Tissue (GFT coated with TiO₂), suitable for photocatalysis-plasma processes, was investigated for Butane-2,3-dione and Heptan-2-one degradation under photocatalysis, Dielectric Barrier Discharge (DBD) plasma and by coupling both. Photocatalytic degradation performance was monitored in continuous reactor, for various operating conditions like flowrates, VOCs concentration and complex air flow (mixture of Butane-2,3-dione and Heptan-2-one). Humidity tests were performed to evaluate the efficiency of Butane-2,3-dione/Heptan-2-one removals under photocatalytic oxidation. The integration of DBD plasma treatment in photocatalytic reactor was investigated in order to improve indoor air quality. Good mineralization and an improvement on VOCs destruction were observed resulting in synergies between two oxidation techniques, as well as the formation of oxidized by-products was controlled for mixture treatment.

2. Materials and methods

2.1. Experimental setup

VOCs oxidation runs using a photocatalytic reactor and/or DBD plasma reactor were conducted using the experimental setup shown in Figure 1. It consists of a glass annular reactor (2 concentric Pyrex cylinders, 100 cm length), one outer cylinder of 76 mm and an inner cylinder of 58 mm with wall thickness of 4 mm. The reactor can be used in a photocatalytic mode via UV lamp (Philips TL 40W/05) and/or in a plasma mode (Dielectric Barrier Discharge DBD system) or in a simultaneous mode. Experiments were realized at ambient temperature (25°C) and atmospheric pressure. In order to have a homogeneous irradiation on the total catalyst surface, a UV lamp (100 cm length) was placed in the inner concentric cylinder. A commercial Glass Fiber Tissue TiO₂/GFT (BET surface: 300 m² g⁻¹, diameter: 5-10 nm, Anatase 100%), produced by Ahlstrom Research and Services, was used as catalyst. As for DBD plasma equipment, Figure 1. shows the different experimental parts used to create the plasma. DBD plasma was created by applying high voltage power via a signal generator (BFI OPTILAS (SRS) reference DS 335/1). The applied voltage, as a sinusoidal waveform of 10V, was then amplified to 30 kV by an amplifier (TREK 30A/40) [20, 22-25]. This amplifier is connected to the reactor outer/inner electrodes, in a copper and Al grid form for the outer and inner electrodes, respectively. The voltages applied in the plasma reactor are measured by high-voltage probes recorded with a digital oscilloscope (Lecroy wave surfer 24Xs, 200 MHz).

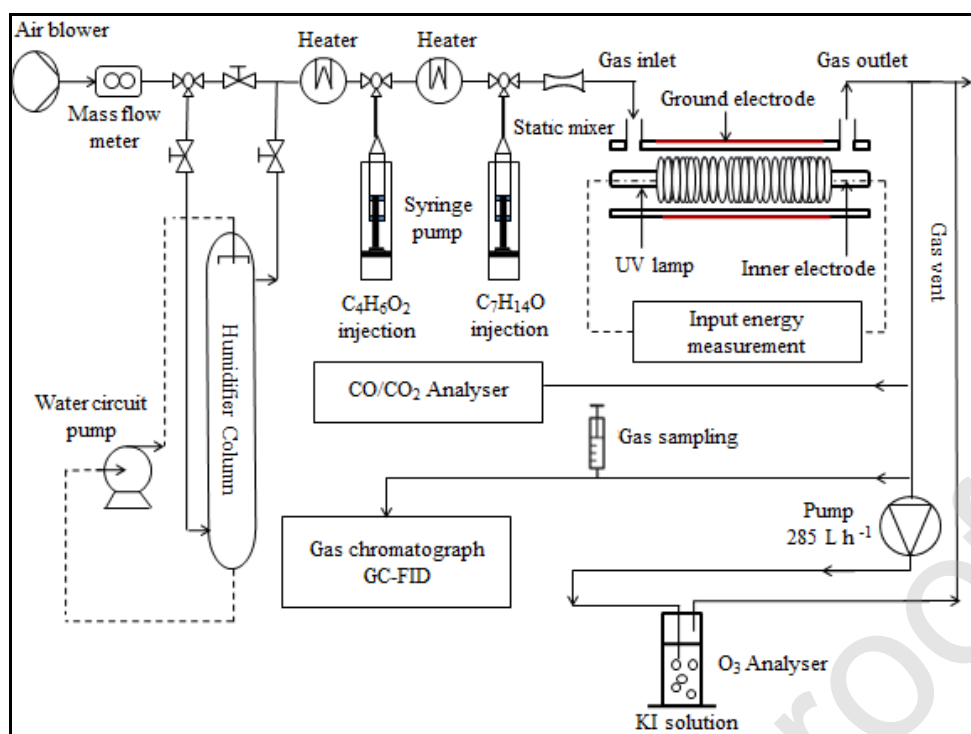


Figure 1. Schematic of the experimental setup: abatement of VOCs in air mixture system.

2.2. VOC injection

Two organic compounds: Butane-2,3-dione (diketone, two C=O groups) and Heptan-2-one (ketone groups) were used. The Butane-2,3-dione ($C_4H_6O_2$) 99% purity was purchased from Janssen Chimica. As for Heptan-2-one, ($C_7H_{14}O$, 98% purity) was supplied from Acros Organics. The polluted air flow was generated continuously by means of a syringe pump system (Kd Scientific Model 100). In order to create a complex air flow, two similar injection systems are used for each compound (Figure 1). A static mixer upstream ensures a good mixture of the complex Butane-2,3-dione/Heptan-2-one. A set of valves and a flow controller (Bronkhorst In-Flow) ensured a variable input flow (from 1 to 10 $m^3 h^{-1}$) into the reactor. Relative Humidity (RH) can also be modified. A variable fraction of gas stream came from a humidifier packed column to obtain humidity ranges from 40 to 90%. Humidity and temperature

in the inlet of photocatalytic/plasma reactor were monitored via a specific sensor (Testo 445).

2.3. Analysis system

2.3.1. VOC analysis

Gas Chromatography (GC), equipped with a flame ionization detector (FID), was used to monitor the evolution of VOCs over time. The analysis was carried out using a Clarus GC-500 chromatograph equipped with a 60 m × 0.25 mm polar DB-MS capillary column (film thickness, 0.25 μm). The detector (FID) is powered by a mixture of air and hydrogen (H₂). Helium (He) was used as a carrier gas at a flow rate of 1 ml min⁻¹. The samples (500 μL) are injected manually via a gas syringe. Analysis conditions, as injection detection temperatures (250°C for both), were used to quantify INLET/OUTLET VOC concentrations. Oven temperature, initially kept at 50°C for 3 min, was programmed to rise from 50 to 100°C at 2°C/min, remaining at the maximum temperature for 10 min thereafter.

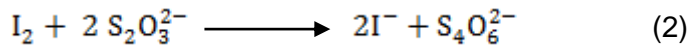
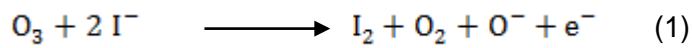
2.3.2. CO and CO₂ analysis

The measurement of the amount of CO₂ produced during C₄H₆O₂/C₇H₁₄O treatment was carried out on an online analytical system via a Fourier Transform Infrared Spectrophotometer (FTIR) of Environment SA (MIR 9000H). To monitor the mineralization step continuously during the oxidation test, a pump system of the gas stream was connected to the outlet of the reactor. CO measurement was made at the outlet of the reactor, a gas analyzer NO/CO ZRE marketed by Fuji Electric France S.A.S was connected online.

2.3.3. Ozone analysis

Ozone was generated via DBD plasma step during VOC degradation. The amount of Ozone produced was determined by sodium thiosulfate titration method. Exhaust gas

flow, equal to 285 L h^{-1} , was delivered by a membrane pump (KNF lab N86k18) to a bubbler (500 ml), containing a solution of iodide of potassium (KI, at 10^{-2} M). A chemical reaction between potassium iodide (KI) and Ozone occurs, giving yellow color emerges, as first step (Equation 1) and then it move towards a titration by sodium thiosulphate solution ($\text{Na}_2\text{S}_2\text{O}_3$, at 10^{-3} M), until a colorless solution is obtained, as second step (Equation 2) [24]. The titration is carried out in an acid medium by dripping concentrated sulfuric acid (H_2SO_4) in the final solution.



2.4. Analytic methods

In order to understand the performance of the plasma-photocatalytic reactor, some parameters were monitored as:

- $\text{C}_4\text{H}_6\text{O}_2$ Removal Efficiency:
$$RE (\%) = \frac{([\text{C}_4\text{H}_6\text{O}_2]_{\text{INLET}} - [\text{C}_4\text{H}_6\text{O}_2]_{\text{OUTLET}}) \times 100}{[\text{C}_4\text{H}_6\text{O}_2]_{\text{INLET}}} \quad (3)$$

- $\text{C}_7\text{H}_{14}\text{O}$ Removal Efficiency:
$$RE (\%) = \frac{([\text{C}_7\text{H}_{14}\text{O}]_{\text{INLET}} - [\text{C}_7\text{H}_{14}\text{O}]_{\text{OUTLET}}) \times 100}{[\text{C}_7\text{H}_{14}\text{O}]_{\text{INLET}}} \quad (4)$$

- Specific Input Energy:
$$SIE (\text{J L}^{-1}) = \frac{3600 \times P}{Q \times 1000} \quad (5)$$

With: P (W) is input power adjusted by changing the applied voltage (U_a) at a constant frequency (50 Hz) and Q ($\text{m}^3 \text{ h}^{-1}$) is the flowrate tested. $[\text{VOCs}]_{\text{INLET}}$, $[\text{VOCs}]_{\text{OUTLET}}$ are the INLET/OUTLET gas mass concentrations, respectively.

- Elimination Capacity:
$$EC (\text{mg h}^{-1}) = \frac{RE (\%) \times [\text{VOCs}]_{\text{INLET}} \times Q}{100} \quad (6)$$

- Selectivity of CO:
$$SCO (\%) = \frac{[\text{CO}]_{\text{OUTLET}} - [\text{CO}]_{\text{INLET}}}{N_C \times RE (\%) \times [\text{VOCs}]_{\text{INLET}}} * 10000 \quad (7)$$

- Selectivity of CO_2 :
$$SCO_2 (\%) = \frac{[\text{CO}_2]_{\text{OUTLET}} - [\text{CO}_2]_{\text{INLET}}}{N_C \times RE (\%) \times [\text{VOCs}]_{\text{INLET}}} * 10000 \quad (8)$$

3. Results and discussion

3.1. VOC removal under photocatalysis alone

Single compounds

3.1.1. Effects of flow rate & VOC concentration

Firstly, the performance of the photocatalytic oxidation process was studied on two separate VOCs: Butane-2,3-dione/Heptan-2-one, treated alone. Figure 2 shows the variation of the removal efficiency at variable concentrations (ranging from 5 to 27 mg m^{-3}) and for two flow rates (2 and 4 $\text{m}^3 \text{h}^{-1}$), all experiments on $\text{C}_4\text{H}_6\text{O}_2$ and $\text{C}_7\text{H}_{14}\text{O}$ removal were realized under a dry condition ($\text{RH} \sim 5\%$). As shown in Figure 2, increasing the inlet concentration of VOCs can negatively influence the performance of degradation. At a constant air flow (2 $\text{m}^3 \text{h}^{-1}$), the increase of the $\text{C}_4\text{H}_6\text{O}_2$ amount from 5 to 20 mg m^{-3} , results in a decrease of the degradation rate from 74.75 to 44.93%. Our previous studies confirm this behavior and relate this decrease to the saturation/deactivation of the active sites of catalyst [12,18, 20]. In addition, it was found (Fig. 2), that the oxidation performance was clearly decreased by increasing the flow of air/VOCs. The decrease is largely due to the short contact time between VOCs/catalyst, which leads to influence the removal capacity. Regarding Heptan-2-one behavior, the same trend was observed on the degradation. However, it is important to note that the degradation rate for $\text{C}_7\text{H}_{14}\text{O}$ remains low ($\sim 32.41\%$ at 2 $\text{m}^3 \text{h}^{-1}$) compared to Butane-2,3-dione ($\sim 74.75\%$ at 2 $\text{m}^3 \text{h}^{-1}$). Heptan-2-one presents a long molecular chain ($\text{C}_7\text{H}_{14}\text{O}$), harder to degrade using photocatalytic treatment, which explains the decreasing trend of the efficiency.

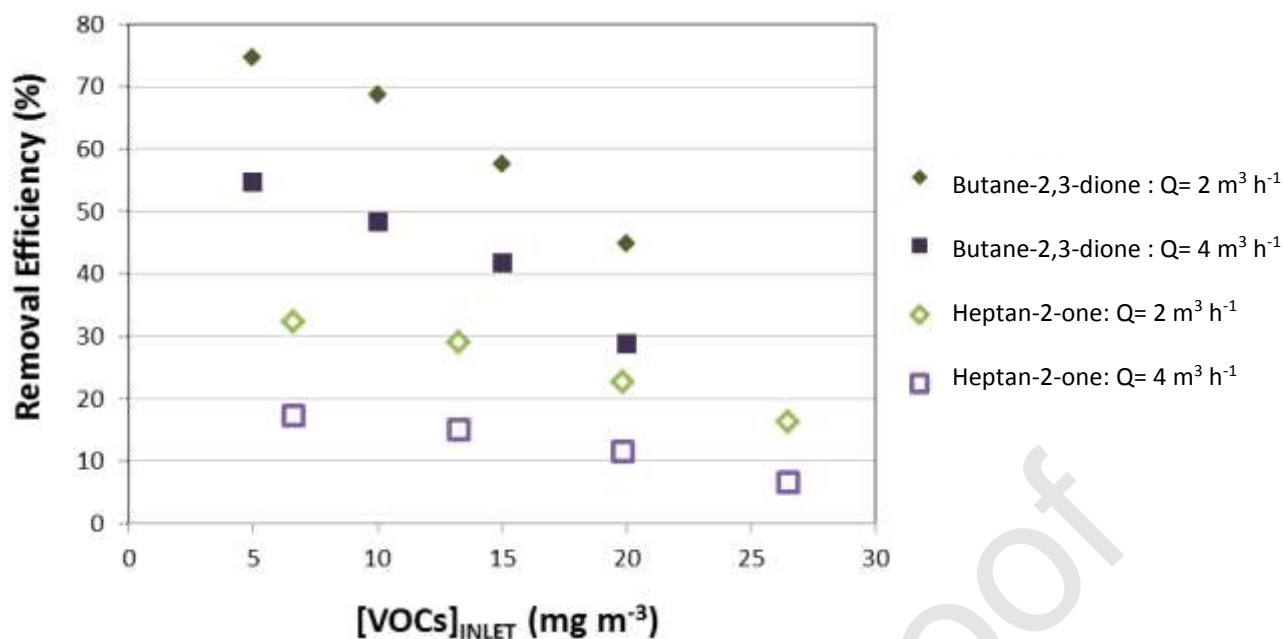


Figure 2. Variation of the removal efficiency of Butane-2,3-dione and Heptan-2-one with inlet concentration at different flow rates using photocatalysis.

(T= 25 °C, UV intensity= 20 W m⁻², RH= 5%)

3.1.2. Effect of humidity on VOC removal

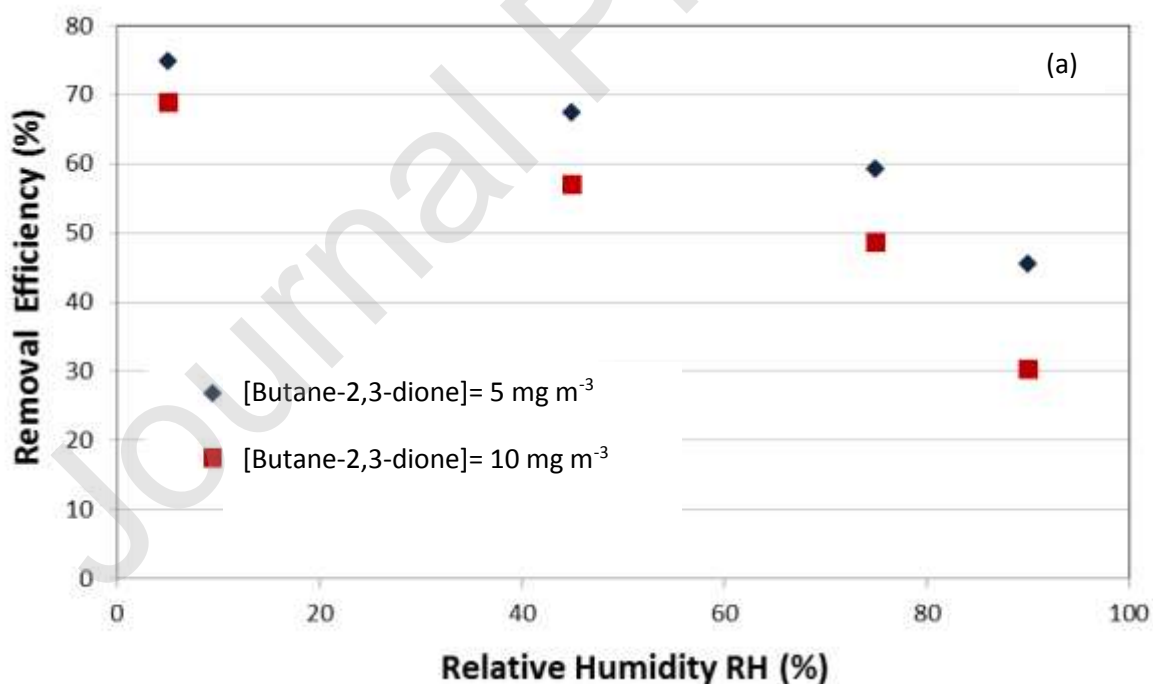
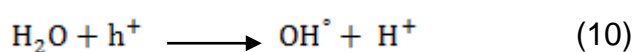
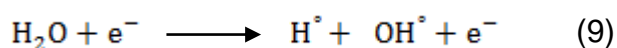
Indoor air in the food industry is usually humid (around 75-95% relative humidity (RH)) [26]; therefore, to simulate real operating conditions in the industrial sector, the photocatalytic reactor was fed with a continuous humid air flow at a rate of 2 m³ h⁻¹ and at various humidity values. Figure 3 shows the variation of the removal efficiency, at four values of relative humidity (~5%, ~45%, ~75% and ~90% RH), of (a) Butane-2,3-dione and (b) Heptan-2-one with two different inlet concentrations like 5-10 mg m⁻³ and 6.6-13.25 mg m⁻³, respectively. Different behaviors were observed during the photocatalytic degradation of both VOCs treated separately. Regarding the influence of humidity on the Butane-2,3-dione degradation, a result (Figure 3 (a)) shows that the removal efficiency was significantly affected by increasing relative humidity from 5% to 90%, for both 5 and 10 mg m⁻³ of Butane-2,3-dione. For

example, the experiment realized at low humidity (RH ~ 5%) at $[C_4H_6O_2]= 10 \text{ mg m}^{-3}$, Butane-2,3-dione removal was 68.79% and gradually decreased to become 56.9%, 48.56% and 30.32% with ~ 45%, ~ 75% and ~ 90% of the humidity levels, respectively. Thus, the effect of the competitive adsorption on the catalyst active sites between the water vapor molecules (H_2O), the butane-2,3-dione ($C_4H_6O_2$) and its oxidation by-products is present whatever the relative humidity value is. In addition to that, the higher the humidity, the more there is deactivation of catalyst active sites. As a result, a permanent decrease in the butane-2,3-dione removal efficiency is observed due to the water vapor amount increase. As for Heptan-2-one, the same previous methodology was used and the results are shown in Figure 3 (b). A different behavior was observed in comparison with that previously described on Butane-2,3-dione alone: when the water vapor amount is low, the created active intermediate species help to increase the oxidation of the heptan-2-one ($C_7H_{14}O$) and the effect of the competitive adsorption is neglected. Moreover, this behavior can be attributed to the high molecular weight of $C_7H_{14}O$ compared to $C_4H_6O_2$ which hampers the competitive adsorption and thus improves photocatalytic degradation of heptan-2-one. But when the water vapor amount is more and more higher, the effect of the competitive adsorption becomes more important which causes the heptan-2-one removal decrease. Therefore, the presence of moisture in a gaseous stream can present a double effect on $C_7H_{14}O$ oxidation:

- i. On the one hand, under humid oxidation conditions (from 45 to 75% humidity), the removal efficiency of Heptan-2-one was enhanced. Under dry flow gas (HR ~ 5%) and for an inlet concentration of 6.6 mg m^{-3} , 32.41% of Heptan-2-one was removed and for a humidity level of 75% the degradation rate reached 45.62%. A slight increase in water molecules contributes to generate

hydroxyl radicals OH^\bullet (according to Eq. 9-10), known as highly reactive chemical species, thus helping to ensure a better performance.

- ii. On the other hand, a high level of moisture (RH~90%) leads to increase the competition between water vapor/Heptan-2-one on the catalyst surface and differently affect the degradation efficiency. For the same concentration ($[\text{C}_7\text{H}_{14}\text{O}] = 6.6 \text{ mg m}^{-3}$), it should be noted that at RH~90%, the $\text{C}_7\text{H}_{14}\text{O}$ degradation rate dropped to 38.73% versus 45.62% at RH~75%. These results are in agreement with those reported by Zadi et al., Martinez et al. and Assadi et al. concerning the oxidation of chlorinated VOCs [20], aromatics [27] and aldehydes [25], respectively. The effect of humidity on mixtures was also studied and the results are discussed below (see part 3.1.3., Figure 5).



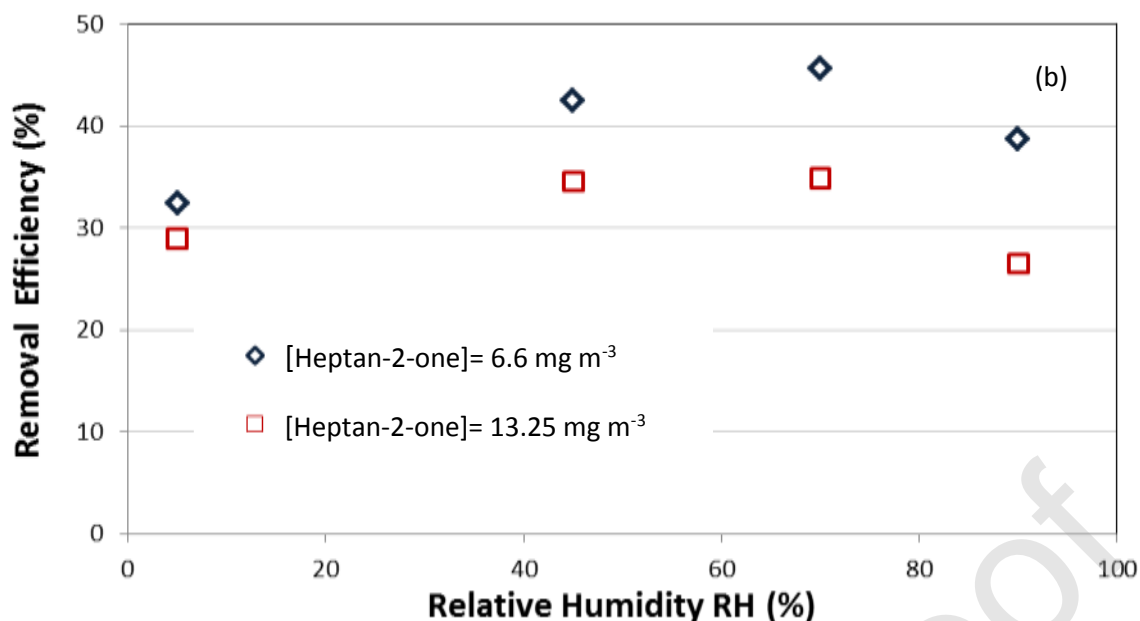


Figure 3. Effect of humidity on (a) Butane-2,3-dione and (b) Heptan-2-one removal efficiencies at different inlet concentrations.

($T = 25\text{ }^{\circ}\text{C}$, UV intensity = 20 Wm^{-2} , $Q_{\text{air}} = 2\text{ m}^3\text{ h}^{-1}$)

Mixture of compounds

3.1.3. Effect of composition of gas

A complex air flow of $\text{C}_4\text{H}_6\text{O}_2$ and $\text{C}_7\text{H}_{14}\text{O}$, at an inlet concentration of 5.2 ppm, was applied using a photocatalytic process for variety molar compositions as (50% Butane-2,3-dione & 50% Heptan-2-one), (25% Butane-2,3-dione & 75% Heptan-2-one) and (75% Butane-2,3-dione & 25% Heptan-2-one). Indeed, the objective of the target molecules mixture study was first to validate the coupled process efficiency in a case more closer to the real conditions where several molecules must be eliminated simultaneously and to see if there is always improvement of pollutants removal in the case of mixing. The objective was also to check the toxicity of the by-products resulting from the oxidation in the case of mixture and to check if new by-products will appear, and the results shows that we obtained the same conventional

by-products (section 3.3.2. below). The flow rate of the mixture stream was set to $2 \text{ m}^3 \text{ h}^{-1}$ and the relative humidity was around 5%. Results of the VOC's elimination capacity are presented in Figure 4. As seen in Figure 3 (a) and 3 (b), relative humidity constitutes an important experimental condition that can differently affect the trend of the photocatalytic VOC degradation. As a consequence, the influence of humidity on $\text{C}_4\text{H}_6\text{O}_2/\text{C}_7\text{H}_{14}\text{O}$ mixture degradation was monitored at 5%, 45% and 90% of relative humidity. These humidity tests are presented in Figure 5. Compared to the monocompound oxidation study (Fig.3 b), a different behavior of $\text{C}_7\text{H}_{14}\text{O}$ degradation was obtained in the case of $\text{C}_4\text{H}_6\text{O}_2/\text{C}_7\text{H}_{14}\text{O}$ mixture.

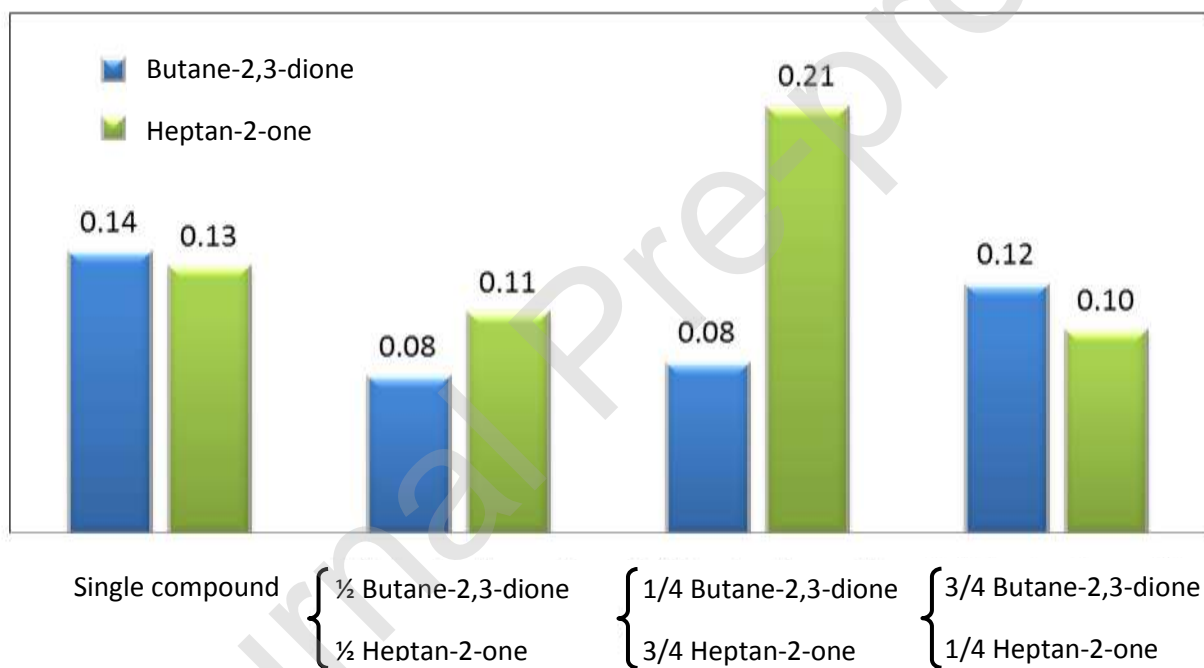


Figure 4. Variation of the elimination rates of $\text{C}_4\text{H}_6\text{O}_2$ alone, $\text{C}_7\text{H}_{14}\text{O}$ alone and binary mixture: under photocatalytic process.

($Q = 2 \text{ m}^3 \text{ h}^{-1}$, $[\text{Mixture}] = [\text{C}_4\text{H}_6\text{O}_2] = [\text{C}_7\text{H}_{14}\text{O}] = 5.2 \text{ ppm}$, $\text{RH} = 5\%$)

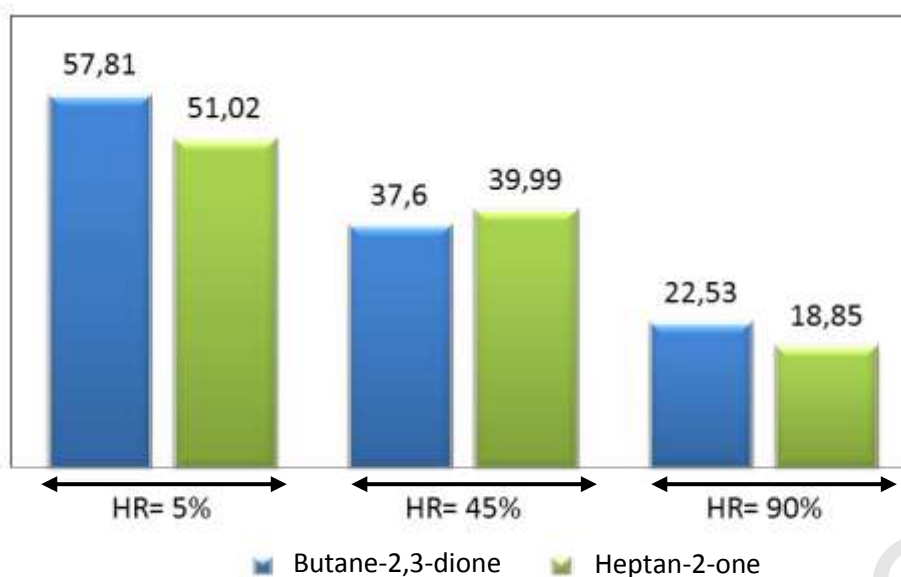


Figure 5. Variation of the removal efficiency of ($C_4H_6O_2/C_7H_{14}O$, 50%-50%) mixture at different values of relative humidity: under photocatalytic process.

($Q=2 \text{ m}^3 \text{ h}^{-1}$, [Mixture]= 5.2 ppm, RH= 5%)

3.2. VOC removal under DBD plasma alone

VOC removal experiments are detailed in our previous studies, [12,18,25,28-30] either via plasma technology alone or via coupling plasma/photocatalysis indicate that a significant amount of exhaust ozone was produced by increasing energy supplied to plasma. In this context and to avoid very high ozone level generation, experiments have been carried out on a range of specific input energies ranging from 2 to 10 J L^{-1} . DBD plasma tests were realized in the same continuous reactor under a dry condition. The gas stream was fixed at $2 \text{ m}^3 \text{ h}^{-1}$ and the $C_4H_6O_2$ concentration was 10 mg m^{-3} . The $C_4H_6O_2$ removal efficiency via DBD reactor was studied and the results are reported in Figure 6. A positive effect of the Specific Input Energy (SIE) increase on $C_4H_6O_2$ oxidation was observed. At higher energy values, a larger quantity of reactive species was formed in the discharge phase like atoms, ions, radicals and metastables, can contribute to enhance VOC degradation by different

ways (atomic oxygen O° , OH° hydroxyl radicals, HO_2° hydroperoxyl radicals, ozone O_3 , N° radicals...) [2,8,31-34]. Figure 7 compares the degradation behavior of Butane-2,3-dione and Heptan-2-one tested separately via DBD plasma system. The initial concentration of $C_4H_6O_2/C_7H_{14}O$ gazes was 2.6 ppm and at a constant flow rate of $2\text{ m}^3\text{ h}^{-1}$ with 5% of relative humidity. It is readily seen that, by using DBD plasma alone (Fig. 7), the same behavior on removal efficiency was observed as that resulting from photocatalysis alone (Fig. 2). Comparing both ketones, Heptan-2-one is less degradable compared to Butane-2,3-dione. The Heptan-2-one degradation was around 10.48% (at $SIE= 2.25\text{ JL}^{-1}$) and 21.95% (at $SIE= 4.5\text{ JL}^{-1}$), contrast to Butane-2,3-dione when 17.32% and 30.11% was removed for 2.25 and 4.5 JL^{-1} , respectively. These results confirm that the group of molecules, irrespective of the system used, can play an important role in removal efficiency.

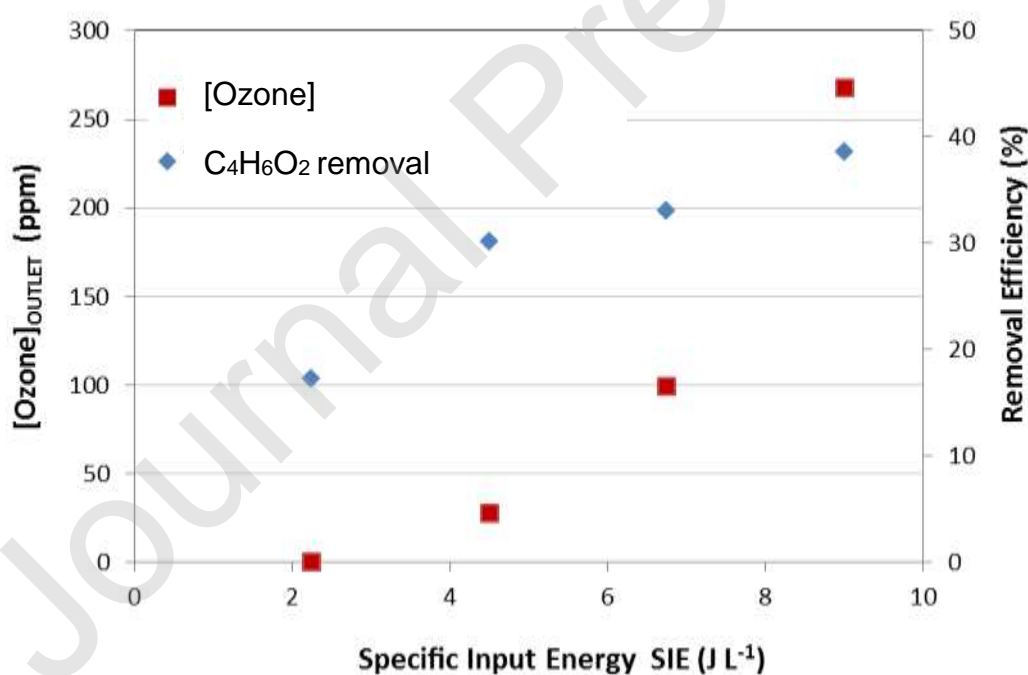


Figure 6. Variation of the removal efficiency of $C_4H_6O_2$ alone and ozone concentration at different values of specific energy: under DBD plasma.

$$(Q= 2\text{ m}^3\text{ h}^{-1}, [C_4H_6O_2]= 10\text{ mg m}^{-3}, RH= 5\%).$$

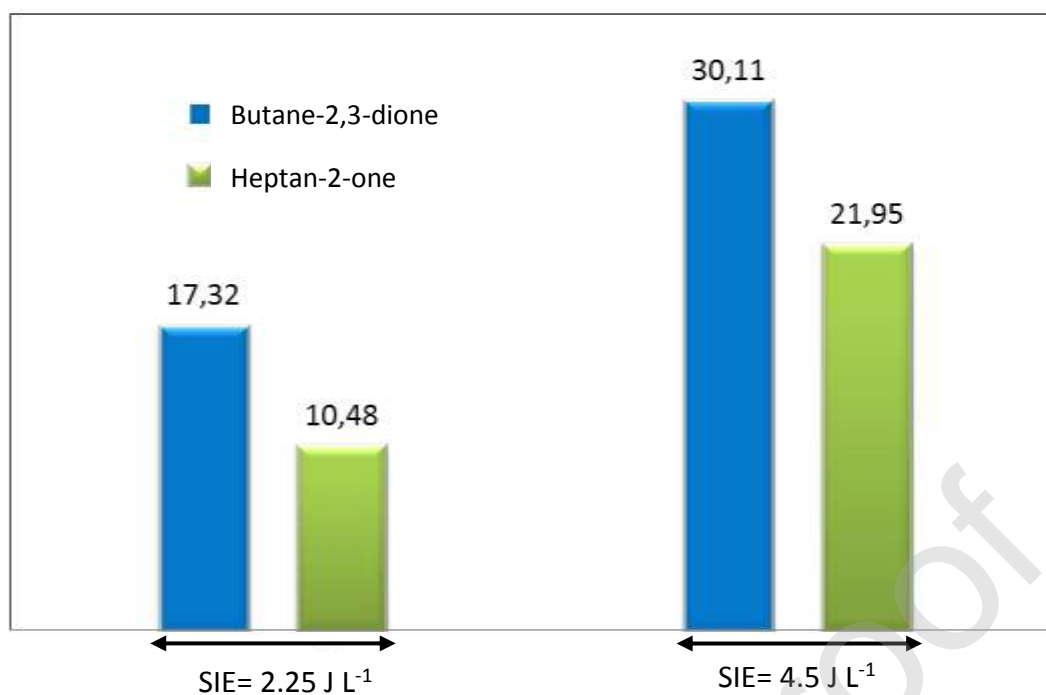


Figure 7. Effect of specific energy on removal efficiency of $C_4H_6O_2$ and $C_7H_{14}O$ treated separately.

($Q=2 \text{ m}^3 \text{ h}^{-1}$, $[C_4H_6O_2]=[C_7H_{14}O]= 2.6 \text{ ppm}$, $RH= 5\%$).

3.3. Application of Photocatalytic/DBD plasma processes

3.3.1. Removal efficiency

The degradation tests of Butane-2,3-dione [100% $C_4H_6O_2$] ~ 5.2 ppm, Heptan-2-one [100% $C_7H_{14}O$] ~ 5.2 ppm, and their equimolar mixture ([VOCs mixture] ~ 5.2 ppm) were studied via photocatalysis, DBD plasma and photocatalytic/DBD plasma processes. Figure 8 compares the evolution of the removal efficiency for single and mixture compounds condition. Coupling plasma-photocatalysis in the same system is more effective for the oxidation of both VOCs (Fig. 8). Either for $C_4H_6O_2$ or $C_7H_{14}O$ oxidation tests, the performance of the degradation was significantly improved via photocatalytic/DBD plasma system. The results for $C_4H_6O_2$ removal by coupling plasma-photocatalysis compared to the results obtained by the sum of removal

efficiencies via DBD plasma test alone and photocatalytic test alone were 63.39% and 62.11%, respectively. As for $C_7H_{14}O$ degradation study, 5.09% was obtained by plasma, 24.39% by photocatalysis and 35.15% by their association. This good synergy observed between cold plasma and photocatalysis is in agreement with other studies for butyraldehyde removal [25,29] and for methane, propene and toluene oxidation [35]. Synergetic effects mainly occur thanks to the important role of generated plasma species which enhance photocatalytic reaction by desorption of oxidation byproducts. The best improvement in this study is 5.7%, but this is simply because the energy applied to the plasma is low (only 4.5 JL^{-1}). We have shown in our previous studies [12,18,20,21,29,30] that the COV removal efficiency is clearly improved by coupling plasma and photocatalysis when using higher energies, but the use of high energy generates a significant amount of ozone [25], which is not desired in our current case of indoor air treatment.

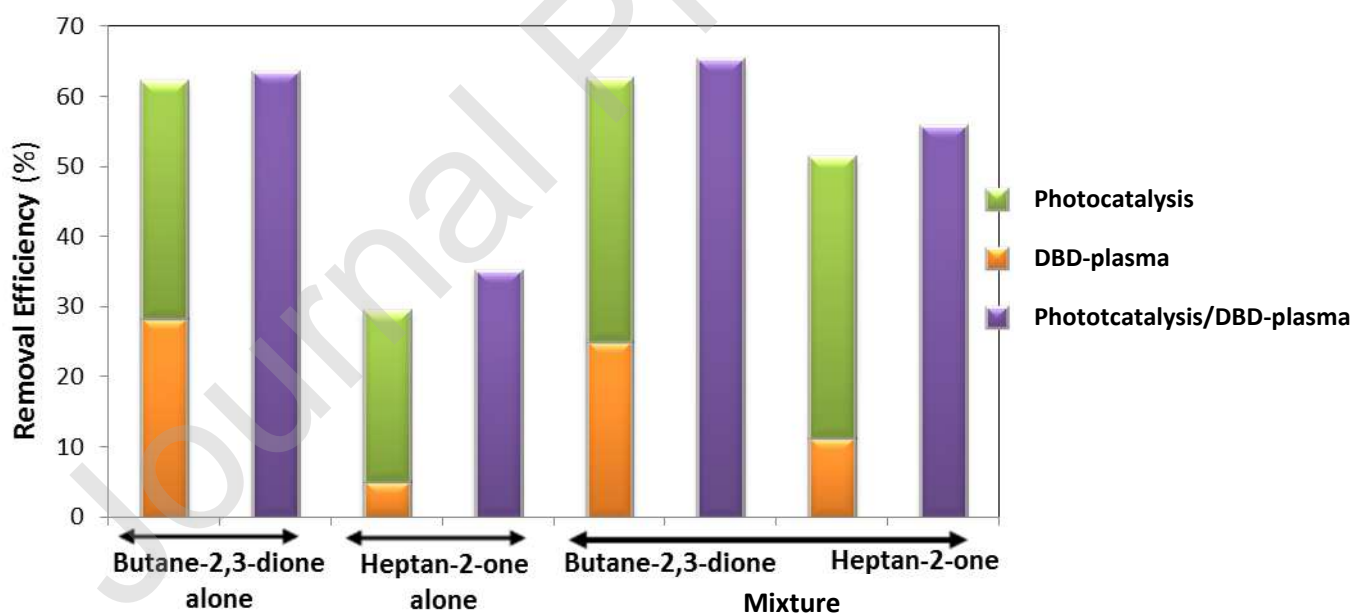
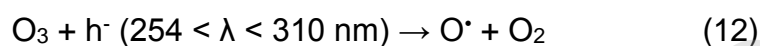


Figure 8. Variation of the removal efficiency of $C_4H_6O_2$, $C_7H_{14}O$, and their mixture using the three oxidation technologies.

($Q=2 \text{ m}^3 \text{ h}^{-1}$, [Mixture]= $[\text{C}_4\text{H}_6\text{O}_2]= [\text{C}_7\text{H}_{14}\text{O}]= 5.2 \text{ ppm}$, $\text{SIE}_{\text{plasma}}=4.5 \text{ JL}^{-1}$, $\text{RH}= 45\%$).

3.3.2. Mineralization, Ozone and by-product formation

Ozone can be seen as a by-product either in plasma treatment or in photocatalytic/plasma treatment; zero ozone was observed during photocatalytic treatment alone (Figure 9). Results show that the quantity of ozone (13.52 mg m^{-3} at the reactor outlet) under photocatalytic/plasma oxidation was decreased compared to ozone produced under the plasma technique (33.80 mg m^{-3}). This amount of ozone reacted on the surface of the catalyst and served to improve the oxidation as shown on the mechanism figure (Fig. 11 below). This reduction presents the positive effect of UV irradiation on ozone decomposition into active species [36].



As for the mineralization step, CO and CO₂ selectivity were monitored for photocatalysis, plasma and coupling of both. According to the Figure 9, it is notable that the selectivity of CO₂ was improved (CO₂ ~ 70.79%), when using plasma-photocatalysis as oxidation process to degrade C₄H₆O₂ and C₇H₁₄O in a mixture system. Oxidation by-products created during C₄H₆O₂/C₇H₁₄O mixture degradation by photocatalysis alone, plasma alone and the association of both was identified by Gas Chromatography coupled to Mass Spectrometry (GC-MS). Outlet oxidation reaction samples were concentrated on a Carbotrap (25ml) and then removed by a thermal desorption unit coupled with GC-MS. Specific oxidation by-products are identified in Figure 10 i and ii as: (1) acetone (C₃H₆O) and acetaldehyde (C₂H₄O), (2) Butane-2,3-dione (C₄H₆O₂), (3) Heptan-2-one (C₇H₁₄O), (4) acetic acid (C₂H₄O₂), (5) formic acid (CH₂O₂), propionic acid (C₃H₆O₂), butanoic acid (C₄H₈O₂), pentanoic acid (C₅H₁₀O₂), hexanoic acid (C₆H₁₂O₂) and Heptane-2,6-dione (C₇H₁₂O₂). Results indicate that the

amount of pollutants (Fig. 10 i): Butane-2,3-dione (2: peak at 4.83 min) and Heptan-2-one (3: peak at 9.61 min) decreased at the outlet of plasma-photocatalytic reactor (a), plasma reactor (b) and photocatalytic reactor (c) respectively, and the amount of the oxidation by-products (Fig. 10 ii) increased by moving from photocatalysis treatment to a plasma-photocatalysis system. A different reaction pathway can take place under combination system: Highly efficient on CO₂ mineralization and more acid compounds were generated. The synergistic mechanism for Butane-2,3-dione & Heptan-2-one degradation when applying simultaneously DBD-plasma and photocatalysis processes is suggested in Figure 11. VOCs: C₄H₆O₂/C₇H₁₄O, Ozone (O₃) and water vapor (H₂O) suggested to be adsorbed on the TiO₂/GFT surface promoting a surface reaction where O₃/H₂O is decomposed into surface active oxygen species/radicals reacting with Butane-2,3-dione and Heptan-2-one and thus improves the photocatalytic oxidation.

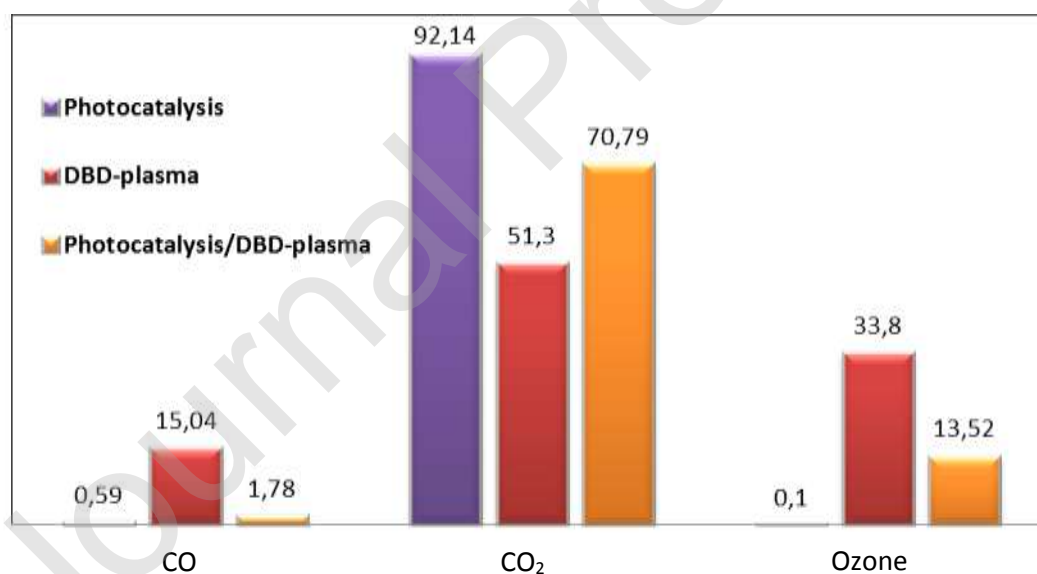


Figure 9. Mineralization rate (%) and ozone concentration (mg m⁻³) via the three oxidation technologies.

(Q=2 m³ h⁻¹, [Mixture]= [C₄H₆O₂]= [C₇H₁₄O]= 5.2 ppm, SIE_{plasma}=4.5 JL⁻¹, RH= 45%).

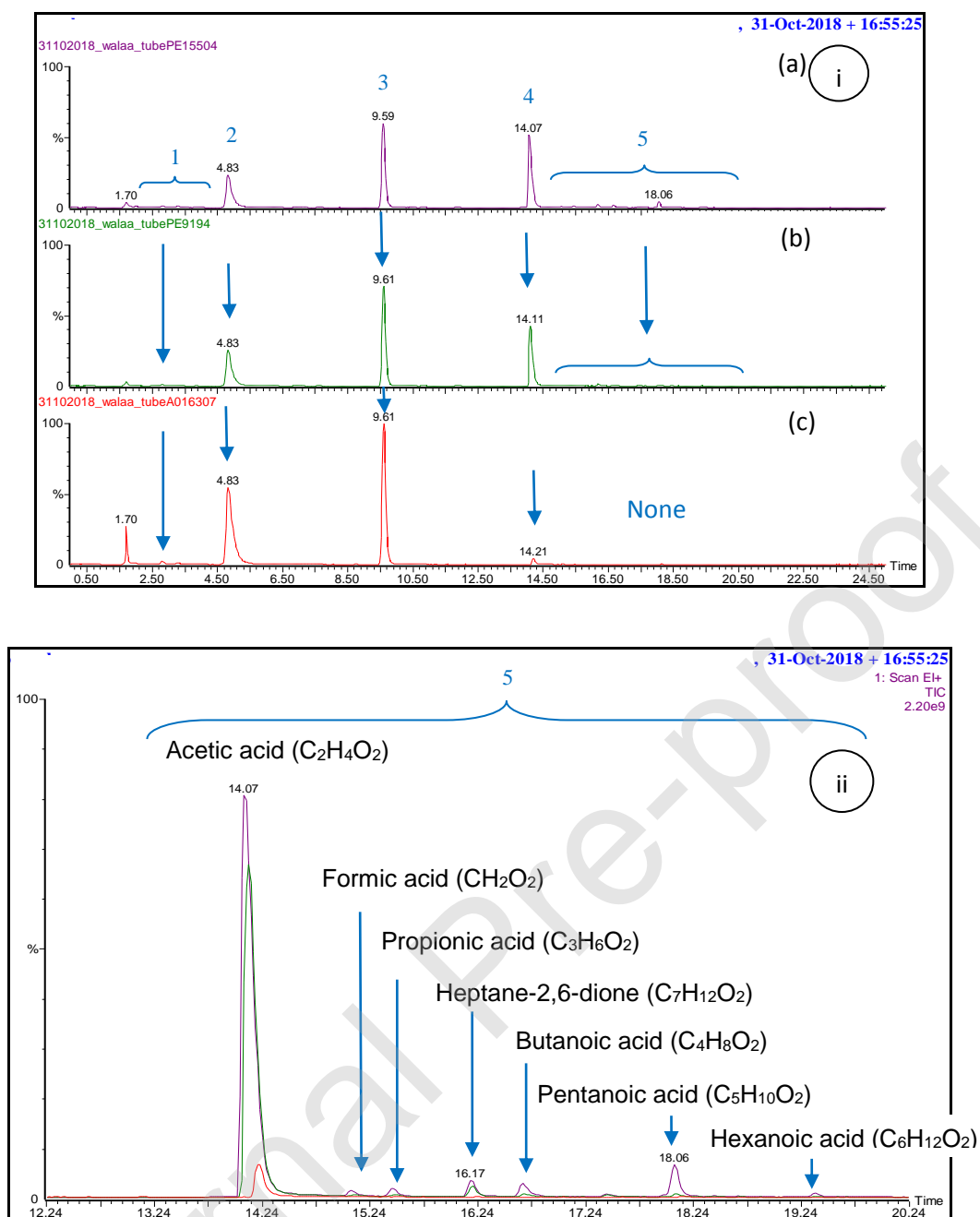


Figure 10. Oxidation by-products identified by GC-MS for $C_4H_6O_2/C_7H_{14}O$ degradation using three oxidation technologies: (a) outlet plasma/photocatalytic reactor, (b) outlet plasma reactor, (c) outlet photocatalytic reactor.

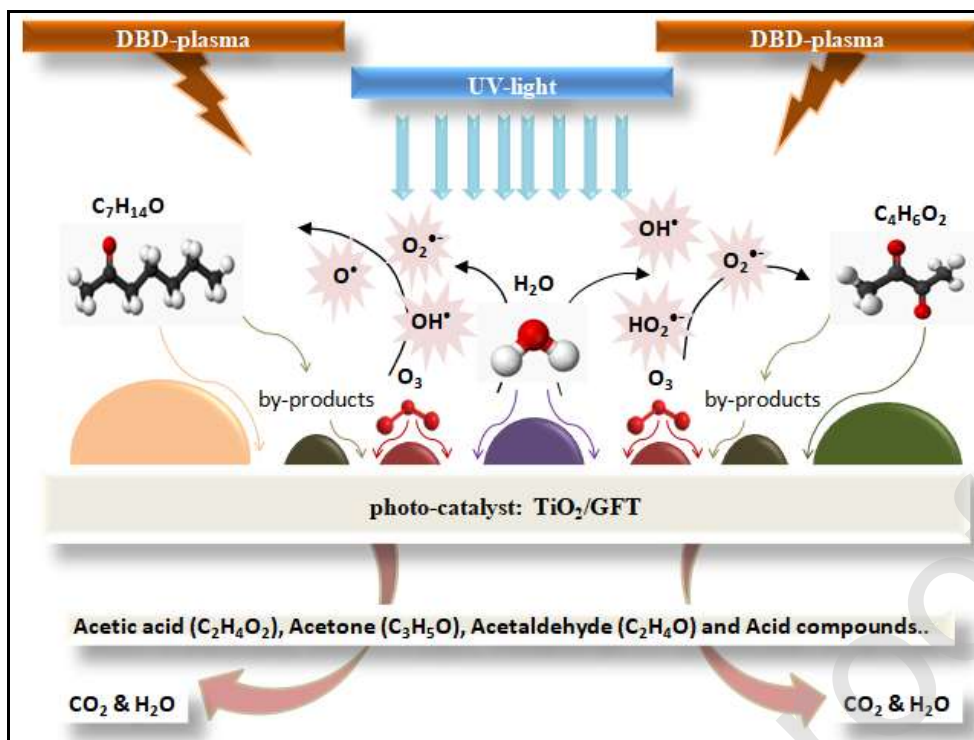


Figure 11. Suggested mechanism for Butane-2,3-dione & Heptan-2-one removal under DBD-plasma/photocatalysis system.

4. Conclusion

Efficiency of photocatalysis, cold plasma and combined both oxidation technologies for the degradation of Butane-2,3-dione and Heptan-2-one as a targets compounds of indoor air pollution were investigated. Photocatalytic performance of a single pollutant was firstly monitored under a variety of experimental conditions: (i) higher flowrate (2 to 4 m³ h⁻¹), (ii) pollutants inlet concentration ranging from 5 to 20 mg m⁻³ and (iii) humidity rate of reaction medium (5 to 90%). Comparing the photocatalytic oxidation of Butane-2,3-dione to that Heptan-2-one, opposite behavior was observed for binary mixture oxidation under humid conditions. Highly efficient synergetic combination was observed in terms of (i) VOC removal efficiency, (ii) CO₂ selectivity and (iii) ozone generation. This system would be useful to limit or eliminate exposure of food industry workers to these harmful VOCs.

References

- [1] X.L. Cao, M. Sparling, R. Dabeka, Occurrence of 13 volatile organic compounds in foods from the Canadian total diet study, *Food Addit. Contam. Part A Chem. Anal Control Expo. Risk. Assess.* (2016) 373-82.
- [2] F. Holzer, F.D. Kopinke, U. Roland, Non-thermal plasma treatment for the elimination of odorous compounds from exhaust air from cooking processes, *Chem. Eng. J.* (2018) 1988-1995.
- [3] C. Scotto, X. Fernandez, Olfactory pollution in urban environment: special case of odors in restaurants, *POLLUTION ATMOSPHERIQUE N°234 AVRIL-JUIN 2017*.
- [4] Y. Huang, S.S. Hang Ho, Y. Lu, R. Niu, L. Xu, J. Cao, S. Lee, Removal of Indoor Volatile Organic Compounds via Photocatalytic Oxidation: A short Review and Porspect, *Molecules* (2016) 1-20.
- [5] U.L. Rochetto, E. Tomaz, Degradation of volatile organic compounds in the gas phase by heterogenous photocatalysis with titanium dioxide/ultraviolet light, *Journal of the Air & Waste Management Association* (2015) 810-817.
- [6] M. Bahria, F. Haghghata, S. Rohanib, H. Kazemian, Impact of design parameters on the performance of non-thermal plasma air purification system, *Chem. Eng. J.* (2016) 204-212.
- [7] O. Karatum, M.A. Deshusses, A comparative study of dilute VOCs treatment in non-thermal plasma reactor, *Chem. Eng. J.* (2016) 308-315.
- [8] R. Thirumdas, C. Sarangapani, U.S. Annapure, Cold Plasma: A novel Non-Thermal Technology for Food Processing, *Food Biophysics* (2015) 10:1-11.

- [9] F. Rezaei, G. Moussavi, A.R. Bakhtiari, Y. Yamini, Toluene Removal from waste air stream by the catalytic ozonation process with MgO/GAC composite as catalyst, *J. Hazard. Mater.* (2016) 348-358.
- [10] H. Zaitan, M.H. Manero, H. Valdés, Application of high silica zeolite ZSM-5 in a hybrid treatment process based on sequential adsorption and ozonation for VOCs elimination, *Journal of Environmental Sciences* (2016) 59-68.
- [11] C. Guillard, D. Baldassare, C. Duchamp, M.N. Ghazzal, S. Daniele, Photocatalytic degradation and mineralization of a malodorous compound (dimethyl disulfide) using a continuous flow reactor, *Catal. Today* (2007) 160-167.
- [12] W. Abou Saoud, A.A. Assadi, M. Guiza, A. Bouzaza, W. Aboussaoud, A. Ouederni, I. Soutrel, D. Wolbert, S. Rtimi, Study of synergetic effect, catalytic poisoning and regeneration using dielectric barrier discharge and photocatalysis in a continuous reactor: Abatement of pollutants in air mixture system, *Appl. Catal. B Environ.* (2017) 53-61.
- [13] A. Alonso-Tellez, D. Robert, N. Keller, V. Keller, A parametric study of the UV-A photocatalytic oxidation of H₂S over TiO₂, *Appl. Catal. B Environ.* (2012) 209-218.
- [14] M. Schiavon, V. Torretta, A. Casazza, M. Ragazzi, Non-thermal Plasma as an Innovative Option for the Abatement of Volatile Organic Compounds: a Review, *Water Air Soil Pollut* (2017) 228-388.
- [15] N. Jiang, C. Qiu, L. Guo, K. Shang, N. Lu, J. Li, Post plasma-catalysis of low concentration VOC over alumina-supported silver catalysts in a surface/packed-bed hybrid discharge reactor, *Water, Air, & Soil Pollution* (2017a) 228, 113.

- [16] B. Dou, D. Liu, Q. Zhang, R. Zhao, Q. Hao, F. Bin, J. Cao, Enhanced removal of toluene by dielectrical barrier discharge coupling with CU-Ce-Zr supported ZSM-5/TiO₂/Al₂O₃, *Catalysis Communications* (2017) 15-18.
- [17] T. Pham Huu, L. Sivachandiran, P. Da Costa, A. Khacef, Methane, Propene and Toluene Oxidation by Plasma-Pd/c-Al₂O₃ Hybrid Reactor: Investigation of a Synergetic Effect, *Top. Catal.* (2017) 326-332.
- [18] W. Abou Saoud, A.A. Assadi, M. Guiza, A. Bouzaza, W. Aboussaoud, I. Soutrel, A. Ouederni, D. Wolbert, S. Rtimi, Abatement of ammonia and butyraldehyde under non-thermal plasma and photocatalysis: Oxidation processes for the removal of mixture pollutants at pilot scale, *Chem. Eng. J.* (2018) 165-172.
- [19] D. Mei, X. Zhu, C. Wu, B. Ashford, T. Williams Paul, X. Tu, Plasma-photocatalytic conversion of CO₂ at low temperatures: Understanding the synergistic effect of plasma-catalysis, *Appl. Catal. B: Environ.* (2016) 525-532.
- [20] T. Zadi, A.A. Assadi, N. Nasrallah, R. Bouallouche, P.N. Tri, A. Bouzaza, M.M. Azizi, R. Maachi, D. Wolbert, Treatment of hospital indoor air by a hybrid system of combined plasma with photocatalysis: Case of trichloromethane, *Chem. Eng. J.* (2018) 276-286.
- [21] A.A. Assadi, S. Loganathan, N.Tri Phuong, S. Gharib-Abou Ghaida, A. Bouzaza, N.Tuan Anh, D. Wolbert, Pilot scale degradation of mono and multi volatile organic compounds by surface discharge plasma/TiO₂ reactor: investigation of competition and synergism, *J. Hazard. Mater.* (2018) 305-313.
- [22] A.A. Assadi, A. Bouzaza, I. Soutrel, P. Petit, K. Medimagh, D. Wolbert, A study of pollution removal in exhaust gases from animal quartering centers by combining

- photocatalysis with surface discharge plasma: from pilot to industrial scale, *Chem. Eng. Process.* (2017) 1-6.
- [23] G. Costa, A.A. Assadi, S. Gharib-Abou Ghaida, A. Bouzaza, D. Wolbert, Study of butyraldehyde degradation and by-products formation by using a surface plasma discharge in pilot scale: Process modeling and simulation of relative humidity effect, *Chem. Eng. J.* (2017) 785-792.
- [24] M. Guillerm, A.A. Assadi, B. Abdelkrim, W. Dominique, Removal of gas-phase ammonia and hydrogen sulfide using photocatalysis, non thermal plasma, and combined plasma and photocatalysis at pilot scale, *Environ. Sci. Pollut. Res.* (2014) 13127-13137.
- [25] W. Abou Saoud, A. A. Assadi, M. Guiza, S. Loganathan, A. Bouzaza, W. Aboussaoud, A. Ouederni, S. Rtimi, D. Wolbert, Synergism between non-thermal plasma and photocatalysis: Implications in the post discharge of ozone at a pilot scale in a catalytic fixed-bed reactor, *Appl. Catal. B: Environ* (2019) 227-235.
- [26] A. Li, Y. Zhao, D. Jiang, X. Hou, Measurement of temperature, relative humidity, concentration distribution and flow field in four typical Chinese commercial kitchens, *Building and Environment* (2012) 139-150.
- [27] T. Martinez, A. Bertron, G. Escadeillas, E. Ringot, V. Simon, BTEX abatement by photocatalytic TiO₂-bearing coatings applied to cement mortars, *Building and Environment* (2014) 186-192.
- [28] A.A. Assadi, A. Bouzaza, D. Wolbert, Comparative study between laboratory and large pilot scales for VOC's removal from gas streams in continuous flow surface discharge plasma, *Chemical Engineering Research and Design* (2016) 308-314.

- [29] S. Gharib-Abou Ghaida, A.A. Assadi, G. Costa, A. Bouzaza, D. Wolbert, Association of surface dielectric barrier discharge and photocatalysis in continuous reactor at pilot scale: Butyraldehyde oxidation, by-products identification and ozone valorization, *Chem. Eng. J.* (2016) 276-283.
- [30] A.A. Assadi, S. Loganathan, N. Tri Phuong, S. Gharib-Abou Ghaida, A. Bouzaza, N. Tuan Anh, D. Wolbert, Pilot scale degradation of mono and multi volatile organic compounds by surface discharge plasma/TiO₂ reactor: investigation of competition and synergism, *J. Hazard. Mater.* (2018) 305-313.
- [31] Y. Huang, P. Wang, Z. Wang, Y. Rao, J. Cao, S. Pu, W. Ho, S.C. Lee, Protonated g-C₃N₄/Ti³⁺ self-doped TiO₂ nanocomposite films: Roomtemperature preparation, hydrophilicity, and application for photocatalytic NO_x removal, *Appl. Catal. B: Environ* (2019) 122-131.
- [32] Y. Huang, D. Zhu, Q. Zhang, Y. Zhang, J. Cao, Z. Shen, W. Ho, S.C. Lee, Synthesis of a Bi₂O₂CO₃/ZnFe₂O₄ heterojunction with enhanced photocatalytic activity for visible light irradiation-induced NO removal, *Appl. Catal. B: Environ* (2018) 70-78.
- [33] Y. Huang, Yunxia Gao, Q. Zhang, Y. Zhang, J. Cao, W. Ho, S.C. Lee, Biocompatible FeOOH-Carbon quantum dots nanocomposites for gaseous NO_x removal under visible light: Improved charge separation and High Selectivity, *J. Hazard. Mater.* (2018) 54-62.
- [34] M. Chen, J. Yao, Y. Huang, H. Gong, W. Chu, Enhanced photocatalytic degradation of ciprofloxacin over Bi₂O₃/(BiO)₂CO₃ heterojunctions: Efficiency, kinetics, pathways, mechanisms and toxicity evaluation, *Chem. Eng. J.* (2018) 453-46.

- [35] T. Pham Huu, L. Sivachandiran, P. Da Costa, A. Khacef, Methane, Propene and Toluene Oxidation by Plasma-Pd/c-Al₂O₃ Hybrid Reactor: Investigation of a Synergetic Effect, *Top. Catal.* (2017) 326-332.
- [36] H. Huang, D. Yea, Combination of photocatalysis downstream the non-thermal plasma reactor for oxidation of gas-phase toluene, *J. Hazard. Mater.* 53 (2009) 535-541.

Journal Pre-proof